Dynamics of the Capacitive-Loaded Push-Pull Parallel-Resonant Converter: Investigation by A SPICE Compatible Average Model

Daniel Edry and Sam Ben-Yaakov*

Fax: +972-7-281340; Email: SBY@BGUEE.BITNET
Department of Electrical and Computer Engineering
Ben-Gurion University of the Negev
P. O. Box 653, Beer-Sheva 84105, ISRAEL

Abstract **- An average model of the Capacitive-Loaded Push-Pull Parallel-Resonant DC-DC Converter (CL-PPRC) was developed and applied to study the static and dynamic behavior of the CL-PPRC. The model is compatible to SPICE and can also be used to derive analytical expressions for the static and small signal dynamic responses. It was found that the dynamics of a CL-PPRC, operating in the Continuous (input) Inductor Current Mode, is similar to that of a Boost converter operating in Discontinuous Mode.**

I. INTRODUCTION

Resonant converter are believed to offer a performance advantage over hard switched PWM converters. One of the difficulties in practical design of resonant converters is the need to handle rather complex mathematical expressions that describe the static and dynamic behavior of resonant mode circuits. In particular, the small signal response, required for the feedback loop design, are often difficult to derive and comprehend [1].

Recent advances in electronic circuit simulation offer an alternative approach to the classical circuit design procedures. A Bode plot, generated by simulation, is equivalent from all practical aspects to an analytical expression since any one of the two can be effectively used as the starting point of the feedback design cycle. Of particular interest are therefore equivalent circuit models that are SPICE compatible. Such models can exploit the built in procedures of modern simulator, freeing thereby the designer from tedious mathematical manipulations. For example, all modern simulators will automatically derive the small signal equivalent circuit required to run AC analysis on both linear and non linear models. Hence, once a large signal model is built the problem of small signal analysis is taken care of automatically. Furthermore, by mimicking the operation of the simulator one can, in fact, derive the analytical expressions of the transfer functions either manually or by a symbolic mathematical software package such as Mathematica [2].

The objective of this study was to develop a SPICE compatible average model for the Capacitive-Loaded Push-Pull Parallel-Resonant DC-DC Converter (CL-PPRC) [3,4]. Once developed and verified against cycle by cycle simulation and experimental results, it was then used to study the static and dynamic response of the CL-PPRC.

II. THE CL-PPRC TOPOLOGY

The basic CL-PPRC [3] power stage of Fig. 1 is built around a push-pull configuration (Q1, Q2) and a resonant network (L_r, C_r). The power stage is driven by a symmetrical square wave (f_S) such that:

$$f_S \leq f_{osc} \qquad (1)$$

where f_{osc} is the self oscillating frequency of the system.

The signal generated by the power stage is coupled to the secondary side via an isolating transformer (T_2 in Fig. 1), rectified and filtered by an RC network. This filter arrangement makes the voltage transfer ratio of the CL-PPRC dependent on the driving frequency (f_S).

For a loaded CL-PPRC (Fig. 1) we distinguish four phases (Fig. 2) : (I) the resonant rise (t_0 - t_1), (II) capacitor charge (t_1 - t_2), (III) resonant fall (t_2 -t_3) and (IV) inductor charge (t_3 - t_4).

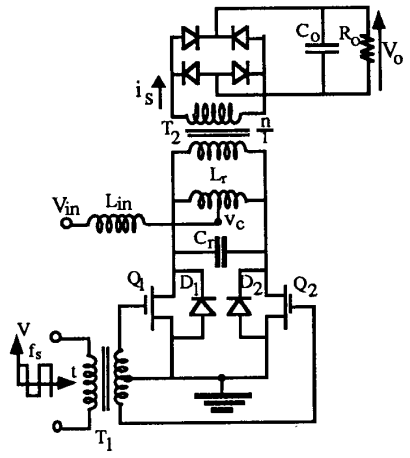

Fig. 1. Basic topology of CL-PPRC.

* Corresponding author. Incumbent of the Luck-Hille Chair of Instrumentation Design.

0-7803-1456-5/94 $4.00 © 1994 IEEE

III. BASIC ANALYTICAL EXPRESSIONS

The analytical expressions for the waveforms has been derived previously [1]. Summarizing the results of the detailed derivation:

$$v_C(t) = \begin{cases} A_1 \mathrm{Sin}(\omega_r(t - t_0)) & ; t \in (t_0 , t_1) \\ A_2 & ; t \in (t_1 , t_2) \\ A_2 \mathrm{Cos}(\omega_r(t - t_2)) & ; t \in (t_2 , t_3) \\ 0 & ; t \in (t_3 , t_4) \end{cases} \quad (2)$$

$$i_L(t) = \begin{cases} I_{in} - A_3 \mathrm{Cos}(\omega_r(t - t_0)) & ; t \in (t_0 , t_1) \\ A_4(t - t_1) + A_5 & ; t \in (t_1 , t_2) \\ I_{in} + A_6 \mathrm{Sin}(\omega_r(t - t_2)) & ; t \in (t_2 , t_3) \\ A_7 & ; t \in (t_3 , t_4) \end{cases} \quad (3)$$

$$i_p(t) = \begin{cases} A_8 - A_4(t - t_1) & ; t \in (t_1 , t_2) \\ 0 & ; \text{elsewhere} \end{cases} \quad (4)$$

where $v_C(t)$, $i_L(t)$ and $i_p(t)$ are the resonant voltage, resonant current and output transformer current, respectively, reflected to the center tap, and:

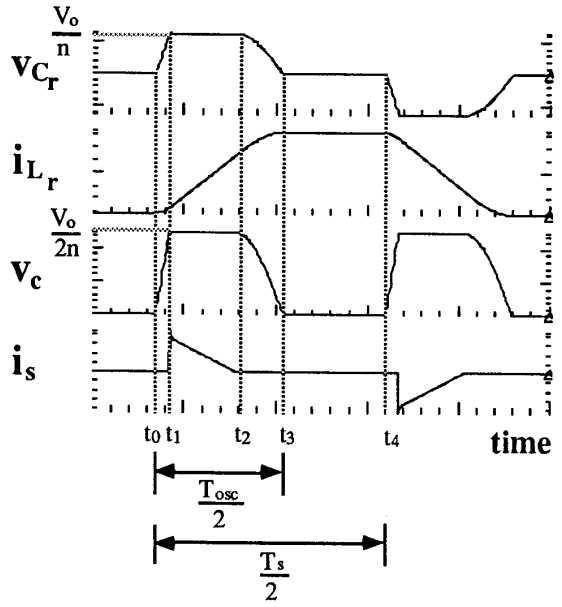

Fig. 2 Expected waveforms of the Capacitive Loaded Push-pull Parallel Resonant Converter (CL-PPRC). See Fig. 1 for notations.

$$A_1 = 2I_{in}Z_r + \frac{V_o}{2n} \quad (5)$$

$$A_2 = \frac{V_o}{2n} \quad (6)$$

$$A_3 = \frac{A_1}{Z_r} = 2I_{in} + \frac{V_o}{2nZ_r} \quad (7)$$

$$A_4 = \frac{A_2}{L} = \frac{V_o}{2nL} \quad (8)$$

$$A_5 = I_{in} - \frac{\sqrt{A_1^2 - A_2^2}}{Z_r} = I_{in} - A_8$$

$$= I_{in} - \sqrt{4I_{in}^2 + \frac{2I_{in}V_o}{nZ_r}} \quad (9)$$

$$A_6 = \frac{V_o}{2nZ_r} \quad (10)$$

$$A_7 = I_{in} + \frac{A_2}{Z_r} = I_{in} + \frac{V_o}{2nZ_r} \quad (11)$$

$$A_8 = \frac{\sqrt{A_1^2 - A_2^2}}{Z_r} = \sqrt{4I_{in}^2 + \frac{2I_{in}V_o}{nZ_r}} \quad (12)$$

$$Z_r = \sqrt{\frac{L}{C}} \quad (13)$$

$$\omega_r = \frac{1}{\sqrt{LC}} \quad (14)$$

$$L = \frac{L_r}{4} \quad (15)$$

$$C = 4C_r \quad (16)$$

The time intervals (Fig. 2) were found by equating the boundary values of the explicit solutions (eq. 2-4) [1]:

$$\Delta t_1 = t_1 - t_0 = \frac{\mathrm{Sin}^{-1}\left(\frac{A_2}{A_1}\right)}{\omega_r} \quad (17)$$

$$\Delta t_2 = t_2 - t_1 = \frac{A_1 \mathrm{Cos}(\omega_r \Delta t_1)}{A_2 Z_r} \quad (18)$$

$$\Delta t_3 = t_3 - t_2 = \frac{\pi}{2\omega_r} \quad (19)$$

$$\Delta t_4 = t_4 - t_3 = \frac{T_s}{2} - (\Delta t_1 + \Delta t_2 + \Delta t_3) \quad (20)$$

IV. THE PROPOSED AVERAGE MODEL

The proposed model for the CL-PPRC (Fig. 3) emulates the basic average behavior by restoring the average voltage across the input inductor and the average current seen by the load. The dependent voltage source E_c (Fig. 3) represents the average voltage seen at the center tap of the resonant network (Fig. 1) and the dependent current source G_s emulates the

average current that flows from the secondary of the transformer (T_2) to the output RC filter (see Figs. 1-3 for notations).

The dependent sources are defined as follows:

$$E_C = \frac{2}{T_S} \int_0^{\frac{T_S}{2}} v_C(t)\,dt \qquad (21)$$

$$G_S = \frac{2}{T_S} \int_0^{\frac{T_S}{2}} i_S(t)\,dt \qquad (22)$$

Where :

$$i_S(t) = \frac{i_p(t)}{2n} \qquad (23)$$

The explicit solutions of the waveform equations (2-20) can now be used to express the analytical relationship between the dependent sources and the parameters of the circuit. To this end we first brake the integral of eq. (21) to the time intervals of the four phases:

$$\int_0^{T_S/2} v_C(t)dt = \int_{t_0}^{t_1} v_{C(I)}(t)dt + \int_{t_1}^{t_2} v_{C(II)}(t)dt + \int_{t_2}^{t_3} v_{C(III)}(t)dt \qquad (24)$$

where :

$$\int_{t_0}^{t_1} v_{C(I)}(t)dt = \int_{t_0}^{t_1} A_1 \mathrm{Sin}(\omega_r t)dt = \frac{A_1}{\omega_r}(1-\mathrm{Cos}(\omega_r \Delta t_1)) \qquad (25)$$

$$\int_{t_1}^{t_2} v_{C(II)}(t)dt = \int_{t_1}^{t_2} A_2 dt = A_2\Delta t_2 = \frac{A_1}{\omega_r}\mathrm{Cos}(\omega_r \Delta t_1) \qquad (26)$$

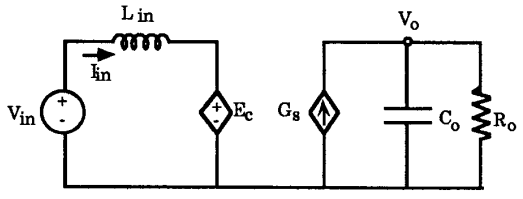

Fig. 3 The core of the proposed average model of the CL-PPRC. E_C and G_S are nonlinear dependent sources.

$$\int_{t_1}^{t_2} v_{C(II)}(t)dt = \int_{t_1}^{t_2} A_2 dt = A_2\Delta t_2 = \frac{A_1}{\omega_r}\mathrm{Cos}(\omega_r \Delta t_1) \qquad (26)$$

$$\int_{t_2}^{t_3} v_{C(III)}(t)dt = \int_{t_2}^{t_3} A_2 \mathrm{Cos}(\omega_r t)dt = \frac{A_2}{\omega_r} \qquad (27)$$

Substituting (25-27) into (24):

$$\int_0^{T_S/2} v_C(t)dt = \frac{A_1 + A_2}{\omega_r} = \frac{\left(2I_{in}Z_r + \frac{V_o}{n}\right)}{\omega_r} \qquad (28)$$

and back into (21):

$$E_C = \frac{2}{T_S}\frac{\left(2I_{in}Z_r + \frac{V_o}{n}\right)}{\omega_r} \qquad (29)$$

using :

$$f_S = \frac{1}{T_S} \quad ; \quad f_r = \frac{\omega_r}{2\pi}$$

we get :

$$E_C = f_S\left(4LI_{in} + \frac{2V_o}{\omega_r n}\right) \qquad (30)$$

The expression for G_S is derived by substituting (4) and (23) into (22):

$$G_S = \frac{f_S}{n}\int_0^{\frac{T_S}{2}} i_p(t)dt = \frac{f_S}{n}\int_{t_1}^{t_2} (A_8 - A_4 t)dt \qquad (31)$$

using the expressions for A_4, A_8 and the time interval Δt_2 (8,12,18), after some rearrangement, we get:

$$G_S = f_S\left(\frac{2}{n\omega_r}I_{in} + 4L\frac{I_{in}^2}{V_o}\right) \qquad (32)$$

Defining :

$$K_1 = \frac{2Z_r}{\pi} = \frac{1}{2\pi}\sqrt{\frac{L_r}{C_r}} \qquad (33)$$

$$K_2 = \frac{1}{n\pi} \qquad (34)$$

and substituting into (21,22) the definitions of the dependent sources simplify to:

$$E_c = \frac{f_s}{f_r}(K_1 I_{in} + K_2 V_o) \tag{35}$$

$$G_s = \frac{f_s}{f_r}\left(K_2 I_{in} + K_1 \frac{I_{in}^2}{V_o}\right) \tag{36}$$

V. SPICE SIMULATIONS

The proposed SPICE compatible model of CL-PPRC (Fig. 4) was built by adding to the core model of Fig. 3 some auxiliary circuitry that emulates the relationships of equations (35-36) (see HSPICE file in the Appendix).

Where :

$$V_{sr} = \frac{f_s}{f_r} \tag{37}$$

$$H_{in} = I_{in} \tag{38}$$

$$E_x = \frac{I_{in}^2}{V_o} = \frac{V_{hin}^2}{V_o} = V_x + V_x V_o - V_{hin}^2 \tag{39}$$

$$E_c = V_{sr}(K_1 V_{hin} + K_2 V_o) \tag{40}$$

$$G_s = V_{sr}(K_2 V_{hin} + K_1 V_x) \tag{41}$$

The independent variable of this circuit is V_{sr} which is the primary driving force. All other voltages and currents are functions of this variable and some constants of the circuit. Notice that the circuit of fig. 4 is for open loop simulations. For closed loop, the source V_{sr} is replaced by a dependent source and the specific circuitry used to close the loop.

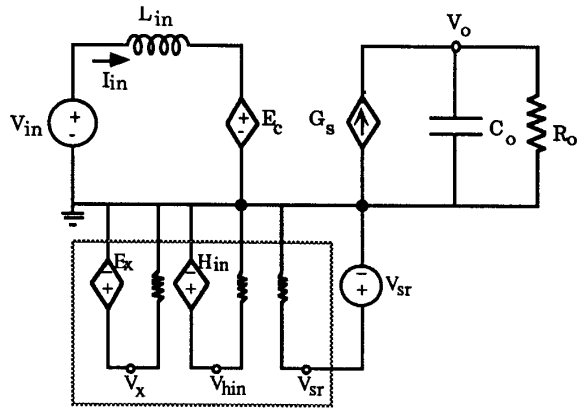

Fig. 4 SPICE compatible model of the CL-PPRC.

VI. DERIVING STATIC AND DYNAMIC RESPONSES

Static response: The analytical expression for the DC transfer ratio of the CL-PPRC can be derived directly from the average model. In steady-state, the voltage across the input inductor must be zero. Hence:

$$E_c = V_{in} \tag{42}$$

Substituting (29) into (42) we get:

$$\frac{f_s}{f_r}\left(\frac{2Z_r}{\pi} I_{in} + \frac{1}{n\pi} V_o\right) = V_{in} \tag{43}$$

Under no-loss condition:

$$I_{in} = \frac{V_o I_o}{V_{in}} = \frac{V_o^2}{V_{in} R_o} \tag{44}$$

Substituting into (43) and rearranging:

$$M^2 + 2nQM - \frac{\pi n^2}{f_s} = 0 \tag{45}$$

where:

$$M = \frac{V_o}{V_{in}} \quad ; \quad Q = \frac{R_o}{4n^2 Z_r}$$

from which the DC transfer ratio of CL-PPRC can be derived to be:

$$M = nQ\left(\sqrt{1 + \frac{2\pi}{Q}\frac{f_r}{f_s}} - 1\right) \tag{46}$$

This expression is identical to the one derived earlier by classical analytical manipulations [3].

Dynamic response: To derive dynamic response expression one has to first define the small signal model. This is done by replacing each of the sources in the average model (Fig. 3) by its differential :

$$d\{E_c\} = f_{sr}(K_1 I_{in} + K_2 V_o) + F_{sr}(K_1 i_{in} + K_2 v_o) \tag{47}$$

$$d\{G_s\} = f_{sr}\left(K_2 I_{in} + K_1 \frac{I_{in}^2}{V_o}\right) + F_{sr}\left(K_2 i_{in} + K_1\left(\frac{2I_{in}}{V_o} i_{in} - \frac{I_{in}^2}{V_o^2} v_o\right)\right) \tag{48}$$

$$d\{V_{in}\} = v_{in} \tag{49}$$

where:

$$F_{sr} = \frac{f_s}{f_r} \tag{50}$$

$$f_{sr} = d\{F_{sr}\} \tag{51}$$

$$v_o = d\{V_o\} \tag{52}$$

$$i_{in} = d\{I_{in}\} \tag{53}$$

The small signal model implies:

$$v_o = d\{G_s\}\, Z_{cr} \tag{54}$$

$$i_{in} = \frac{v_{in} - d\{E_c\}}{Z_L} \tag{55}$$

where :

$$Z_L = sL_{in} \tag{56}$$

$$Z_{cr} = (R_c + \frac{1}{sC_o}) \| R_o = \frac{R_o(1+sC_oR_c)}{1+sC_o(R_c+R_o)} \tag{57}$$

R_c is the ESR of the capacitor C_o and s is the Laplace operator.

Solving (43-44) one gets :

$$\frac{v_o}{f_{sr}}(s) = \frac{A_f\left(1 + \frac{s}{\omega_{z1}}\right)\left(1 - \frac{s}{\omega_{z2}}\right)}{1 + \frac{1}{Q_a}\frac{s}{\omega_o} + \left(\frac{s}{\omega_o}\right)^2} \tag{58}$$

$$\frac{v_o}{v_{in}}(s) = \frac{A_g\left(1 + \frac{s}{\omega_{z1}}\right)}{1 + \frac{1}{Q_a}\frac{s}{\omega_o} + \left(\frac{s}{\omega_o}\right)^2} \tag{59}$$

where:

$$A_f = \frac{R_o(a_1F_{sr}K_1 - a_2a_3)}{F_{sr}K_1(1 + R_oa_4)} \tag{60}$$

$$A_g = \frac{R_oa_4}{F_{sr}K_1(1+R_oa_4)} \tag{61}$$

$$\omega_{z1} = \frac{1}{R_cC_o} \tag{62}$$

$$\omega_{z2} = \frac{a_2a_3 - a_1F_{sr}K_1}{L_{in}a_1} \tag{63}$$

$$\omega_o = \frac{1}{\sqrt{L_{in}C_o(R_o+R_oR_ca_1)}} \tag{64}$$

$$Q_a = \frac{F_{sr}K_1(1+R_oa_4)}{\omega_o(F_{sr}K_1C_o(R_o+R_c)+L_{in}+R_oa_4(L_{in}+F_{sr}K_1R_cC_o))} \tag{65}$$

$$a_1 = K_2I_{in}+K_1\frac{I_{in}^2}{V_o} \tag{66}$$

$$a_2 = F_{sr}\left(K_2+\frac{K_1I_{in}}{V_o}\right) \tag{67}$$

$$a_3 = K_1I_{in}+K_2V_o \tag{68}$$

$$a_4 = K_1K_2F_{sr}^2\left(\frac{I_{in}^2}{V_o}K_2+\frac{2I_{in}}{V_o}\right) \tag{69}$$

VII. RESULTS

The proposed SPICE compatible model was verified by comparing the response of the model to other simulation methods and to experimental results. The nominal values of the experimental converter were L_r=12μH, C_r=10nF, n=26.25, f_s=227KHz, R_o=18KΩ, L_{in}=75μH, C_o=0.033 μF. The switches (IRF640) were driven by two Unitrode drivers UC3705. The system was operated in open loop, applying a home made voltage controlled oscillator (VCO) that was built around a Schmidt trigger (74HCT14). Small signal measurements were made by superimposing an AC signal on a DC level at the input to the VCO. The simulations were carried out on a VAX computer applying the file given in the Appendix. Large signal (time domain) analysis was carried out by running .TRAN analysis while small signal simulation was obtained by .AC analysis on the same (large signal) model.

The static response was verified by comparing the results of model based SPICE simulation to experimental results (Fig. 5). The large signal (time domain) response was verified by

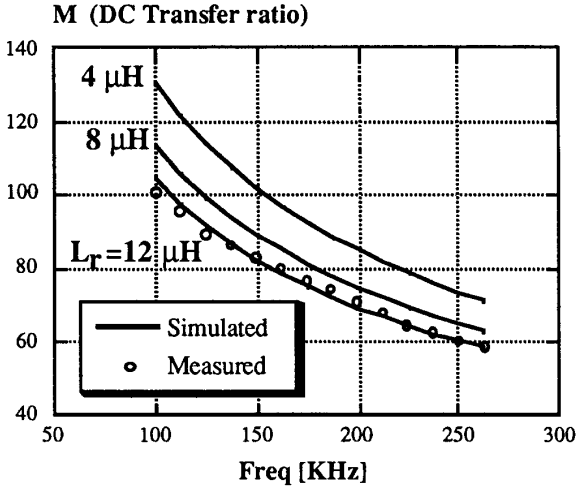

Fig. 5 DC transfer ratio $\left(\frac{V_o}{V_{in}}\right)$ as a function of switching frequency f_s for various values of resonant inductor (L_r).

comparing large signal model based simulation results to those obtained by a straightforward cycle by cycle simulation of the complete CL-PPRC (Fig. 6). The small signal (frequency domain) response was validated by comparing the results of model based SPICE AC analysis to experimental results (Fig. 7). Excellent agreement was obtained in all cases.

VIII. DISCUSSION AND CONCLUSIONS

The present study outlines a methodology for deriving SPICE compatible average models of resonant converters. The SPICE compatible modelling effort is a worthwhile investment since it can alleviate many of the tedious chores involved in the manipulation of complex mathematical expressions. It is further demonstrated that the average modelling approach can also be conveniently used to derive analytical expressions of the static and dynamic responses. It should be emphasized that the model applies only to the case when the CL-PPRC is operating under ZVS and the input current is continuous. The AC analysis (Fig. 8) reveals that the CL-PPRC has a damped double pole response with a Right Half Plane (RHP) zero. Changing the load causes a significant change in the DC gain as well as in the place of the poles and the RHP zero. The small signal output impedance response (Fig. 9) shows a high value at low frequencies and a one pole behavior. This weakness seems to be a significant limitation of the CL-PPRC. However, the AC analysis for the worst case helps to determine the suitable compensation needed for closing the loop. The frequency responses of the experimental converter suggests that a bandwidth of about 5KHz can be achieved by a lag-lead compensator. The initial phase of the control-to-output transfer function (V_o/f_s) is 180 degrees (Fig. 8) due to a negative slope of the DC transfer ratio (M) related to the switching frequency. As has been shown previously [3], the CL-PPRC output voltage (V_o) is almost linear with positive slope related to the switching period (T_s). Therefore, a VCO, in which the period time is linear related to the controlling voltage, would be preferable. The CL-PPRC can be controlled by changing the resonant inductance [6] while keeping the switching frequency without change. This could be very useful for some applications. The proposed average model could be adapted for the new controlling method.

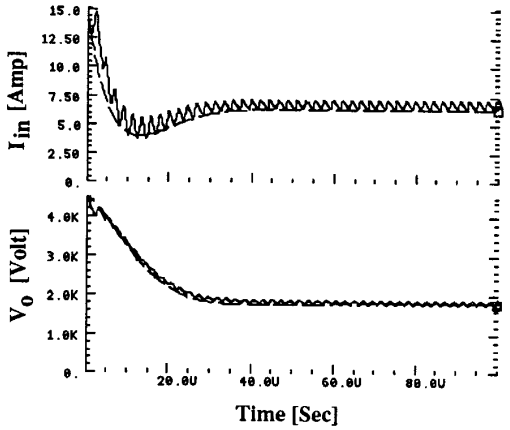

Fig. 6 Transient response by average model simulation (smoothed) vs. cycle by cycle simulation (rippled), for L_{in}=15 μH, C_o=1 nF. Simulations were run on HSPICE [5].

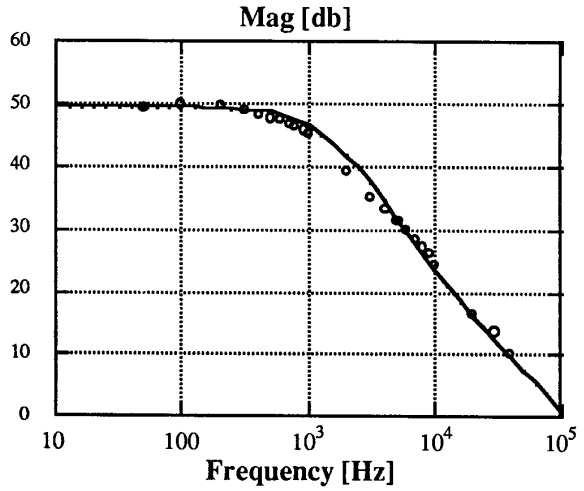

(a)

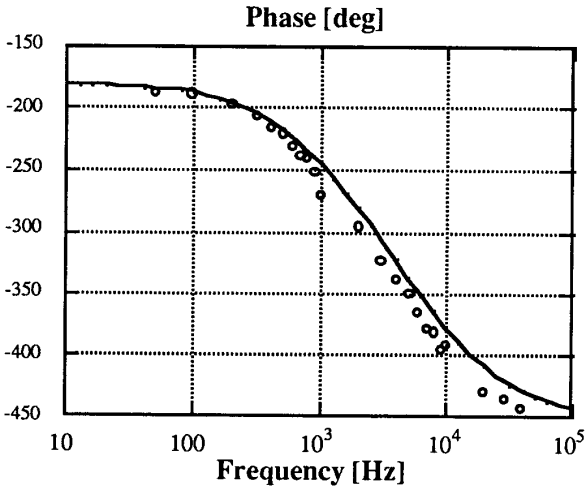

(b)

Fig. 7 Measurements vs. simulations of small signal control to output transfer function. (a) Magnitude (b) Phase. R_o=10KΩ. Simulations were run on HSPICE [5].

IX. APPENDIX

The HSPICE file of the average model for the CL-PPRC is as follows:

```
HVAM3_CL-PPRC_AVERAGE-MODEL
.OPT POST METHOD=GEAR
.PARAM PI=3.14159 LR=12U CR=10N
+ N=26.25 C1='1/2/PI*SQRT(LR/CR)'
+ C2='1/N/PI' FS=227k FR='1/2/PI/SQRT(LR*CR)'
+ RL=18k
VIN 1 0 28
RLIN 1 21 0.1
LIN 21 2 75U IC=15
HIIN 5 0 VIN -1
EC 2 0 POLY(3) 4 0 5 0 3 0
+ 0 0 0 0 0 C1 C2
EX 8 0 POLY(3) 8 0 5 0 3 0
+ 0 1 0 0 0 0 1 -1
GS 0 31 POLY(3) 4 0 5 0 8 0
+ 0 0 0 0 0 C2 C1
VGS 31 32 0
RGS 32 3 7.65
HS 9 0 VGS 1
COUT 3 0 0.0333U IC=1500
ROUT 3 0 RL
* CONTROLLING SOURCE
VSR 4 0 DC 'FS/FR' AC 1
* ANALYSES COMMANDS
.OP
.DC VSR 0.2  0.6  30M
+ SWEEP DATA=DCDATA
.DATA DCDATA LR 12U 8U 4U
.TRAN 1U 500U UIC
.AC DEC 10 1 10MEG
.END
```

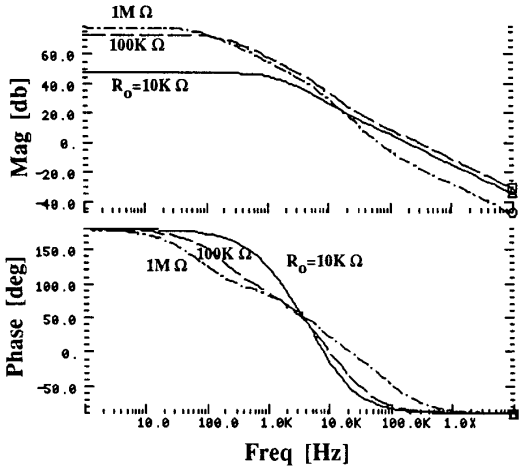

Fig. 8 AC analysis of control-to-output response for various values of output resistor. Simulations were run on HSPICE [5].

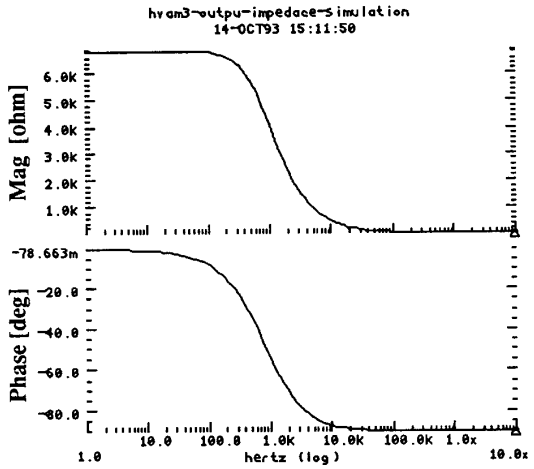

Fig. 9 AC analysis of output impedance of the CL-PPRC for R_O=18KΩ.

REFERENCES

[1] T. Ninomiya, T. Higashi, K. Harada, N. Tsuya, T. Gohnai, and Y. Honda, "Analysis of the static and dynamic characteristics of push-pull parallel resonant converter," *IEEE Power Electronics Specialists Conf. Record*, 1986, 367-374.

[2] S. Wolfram, *Mathematica, a system for doing mathematics by computer*, Addison-Wesley, Redwood City, 1988.

[3] D. Edry, S. Ben-Yaakov, "Capacitive-loaded push-pull parallel resonant converter," APEC conference record, 1993, pp. 51-57. Also in IEEE Trans. on Aero. and Elec. Sys. (in press), to be published in Oct. 1993.

[4] V. Caliscan, J. Gegner and C. Q. Lee, "Current-driven zero-voltage-switched resonant converter with capacitive output filter: Analysis and Experimental results," APEC conference record, 1992, pp. 211-218.

[5] Meta-Software Inc., HSPICE User's Manual, , 1300 White Oaks Road, Campbell, CA 95008.

[6] D. Medini and S. Ben-Yaakov, "A current-controlled variable-inductor for high frequency resonant power circuits," IEEE APEC' 94 (this proceedings).